

# Preparation of $\text{Bi}_4\text{Ti}_3\text{O}_{12}$ (BIT) Ceramics via a High-Energy Ball Milling Process Doped with Multi-Walled Carbon Nanotubes (MWNTs)

Alexandre Gonçalves Pinheiro<sup>1</sup>, Gilberto Dantas Saraiva<sup>1</sup>, Josué Mendes Filho<sup>2</sup>,  
Antonio Sergio Bezerra Sombra<sup>2</sup>

<sup>1</sup>Faculdade de Educação Ciências e Letras do Sertão Central, Universidade Estadual do Ceará, Quixadá, Brazil; <sup>2</sup>Departamento de Física, Universidade Federal do Ceará, Fortaleza, Brazil.

Email: agopin.com@gmail.com

Received June 10<sup>th</sup>, 2013; revised July 22<sup>nd</sup>, 2013; accepted August 9<sup>th</sup>, 2013

Copyright © 2013 Alexandre Gonçalves Pinheiro *et al.* This is an open access article distributed under the Creative Commons Attribution License, which permits unrestricted use, distribution, and reproduction in any medium, provided the original work is properly cited.

## ABSTRACT

We prepared the Nano-sized bismuth titanate  $\text{Bi}_4\text{Ti}_3\text{O}_{12}$  (BIT) powders, through a high-energy ball milling process from their oxides  $\text{Bi}_2\text{O}_3$  and  $\text{TiO}_2$ . This BIT phase can be formed after a milling process for 40 min. With an increasing milling time, this particle size of mixture is gradually reduced, thus, we have mostly an amorphous phase. The BIT ceramics were duly obtained by sintering the synthesized powders at temperatures ranging from 850°C to 1000°C. The BIT ceramics sintered at 1020°C for 1 h, exhibiting a density with 7.52 g/cm<sup>3</sup> of a crystalline phase and a dielectric of  $K = 288.11$  (100 Hz), as well as a dielectric loss of 0.05 (100 kHz). The High-energy ball milling process is a promising way to prepare BIT ceramics. After the preparation of the BIT, we doped it with the Multi-Walled Carbon Nanotubes which are properly obtained by a chemical vapour deposition (CVD), using nickel as a catalyst, as well as using acetylene at 720°C, and then proceeded with the dielectric and optical measurements.

**Keywords:**  $\text{Bi}_4\text{Ti}_3\text{O}_{12}$  Ceramics; Ferroelectric; High-Energy Ball Milling; Sintering; Carbon Nanotubes; MWNT

## 1. Introduction

High K ceramics makes noticeably the miniaturize passive microwave devices. Their sizes can typically be reduced in comparison to the classical resonators and filters by a factor of 1/K (relative dielectric constant). This research work reports the effect of the Multi Wall Carbon Nanotube (MWNT), as a doping of the bismuth titanate  $\text{Bi}_4\text{Ti}_3\text{O}_{12}$  (BIT). Bismuth titanate  $\text{Bi}_4\text{Ti}_3\text{O}_{12}$ , belongs to the family of ferroelectric materials with layered structures, which consists of three perovskite-like units ( $\text{Bi}_4\text{Ti}_3\text{O}_{12}^{2-}$ ), sandwiched between bismuth oxide ( $\text{Bi}_2\text{O}_2^{2+}$ ) layers. BIT single crystals have a low dielectric constant ( $K \sim 244$  at 1 KHz) and a very high Curie temperature ( $T_C = 675^\circ\text{C}$ ), which makes it useful for various applications, such as memory elements, optical displays, piezoelectric and piroelectric devices in a wide temperature range from 20°C to 600°C. Below room temperature it shows an orthorhombic Fmmm symmetry, which exhibits ferroelectric properties [1,2].

BIT ceramics have been used in capacitors, transducers, sensors, etc. [3,4]. The tuning of specific electric properties by compositional modification, as well as the grain size effect, could lead to modifications in the Curie temperature, conductivity, coercivity, compliance, etc. [5,6]. Dielectric properties of BIT ceramics are highly dependent upon the grain size, the phase content in the ceramic body and the sintering temperature. Dielectric constant (K) of BIT ceramics sintered around 850°C, shows values in the range of 235 - 250 with the frequency range of 100 Hz - 100 KHz. The dielectric loss (D) shows a little increase with values around  $1.6 \times 10^{-2}$  in this frequency range [7].

Therefore, ceramics of BIT can show a different dielectric behavior, depending on the particle size. Ferroelectric  $\text{Bi}_4\text{Ti}_3\text{O}_{12}$  (BIT) ceramics are good candidates for the application devices, due to their high dielectric constant, high Curie temperature and high breakdown strength [1-3]. BIT ceramics were conventionally prepared by the solid-state reaction process. The mixture of

Bi<sub>2</sub>O<sub>3</sub> and TiO<sub>2</sub>, was ball milled, calcined at an intermediate temperature and finally sintered at high temperatures [3,4]. This requires a high calcination temperature, usually leading to a particle coarsening and aggregation of the Bi<sub>4</sub>Ti<sub>3</sub>O<sub>12</sub> powders. The presence of hard particle agglomerates will also result both, in poor microstructure and properties of the BIT ceramics. In order to avoid this problem, it is necessary to lower the calcination temperature. The methods reported in the literature to prepare BIT include co-precipitation [5-7] and molten salt synthesis [8]. Wet-chemistry-methods usually involve chemicals (especially its muth salts), which are sensitive to light and other factors. These processes are also very time-consuming. The Mechanochemical process, best known as mechanical alloying or milling [9], has been employed to prepare nano-sized oxides and compounds, such as ZrO<sub>2</sub> [10], Fe<sub>2</sub>O<sub>3</sub> [11], YBCO superconductors [12], magnetic ferrites [13] and ferroelectric powders [14-16]. This mechanical technique is superior to both, the conventional solid-state reaction and the wet-chemistry-based processing in routes with ceramic powders for many reasons: low-cost and widely available oxides as the starting materials, skipping the calcination step at an intermediate temperature, leading to a simplified process [16,17]. The mechanically derived powders possess a much higher sinterability than those powders, synthesized by conventional solid-state reaction and wet-chemical processes.

Multi Wall Carbon Nanotubes, have been of great interest, both from a fundamental point of view and future applications. The most eye-catching features of these structures are their electronic, mechanical, optical and chemical characteristics, which open a wide way for future applications. Nanotube researches have shown possible applications in the fields of energy storage, molecular electronics, nanomechanic devices, and composite materials. Realistic applications are still under development. One of the initial studies in this subject matter, began with carbon nanotubes and it was firstly performed on multi-wall carbon nanotubes (MWNTs), thereafter, two years later on single-wall carbon nanotubes (SWNTs). During the last two decades, many studies on carbon nanotubes, have duly been the subject of many researches, as well. In this particular case, materials were very important, due to the present unique mechanical and electronic properties, which allow an increasing number of applications. The optical and the electronic behaviors of these materials are strongly dependent on the sample size and the morphology, therefore, these properties can be engineered, using hybrid nanoarchitetures [18]. The size-induced quantum confinement in these systems, leads to the observation of a novel phenomena and their striking physical properties, which are being intensively exploited in the nanoscience [19].

This paper is based on a previous one [20]. The present study reports the following: 1) the preparation of nano-sized BIT powders from their oxide mixture, via a ball milling process; 2) ceramics from the synthesized powder will also be presented; 3) Electrical properties of BIT ceramics, doping with multi walled carbon nanotube (MWNT), obtained via the CVD process. In addition, we achieved a faster and a better way to synthesize the BIT orthorhombicphase, therefore, we provided another step to nanotube applications with ferroelectrics composites.

## 2. Experimental Procedure

The commercially available Bi<sub>2</sub>O<sub>3</sub> and TiO<sub>2</sub> powder were used as starting materials for a chemical reaction based on the following:  $2\text{Bi}_2\text{O}_3 + 3\text{TiO}_2 \geq \text{Bi}_4\text{Ti}_3\text{O}_{12}$ .

The above milling experiment was carried out at Fritsch Pulverisette 6 planetary high-energy ball milling system in the air, with room temperatures for different times. A 250 ml stainless steel carbide vial with 10 stainless steel balls, along with a diameter of 20 mm, was used as a milling medium. The milling speed was set at 370 rpm. However, the milling was stopped for 5 min, every 10 min of milling for the cooling down of the system.

The synthesis of the BIT implemented by us (LO-CEM), in shorter times of: milling, calcining and sintering, resulted in a phase that agrees with the literature herewith [21-24]. The procedure described on **Table 1**, shows that we duly obtained the orthorhombic phase, while grinding in a lesser time as in **Figure 1**. The secret to it, was removing dust every 10 minutes of grinding in the walls within the pot, which maximized its reactions and minimized its time, as compared to the X-ray of the BIT and the others [22] (**Figure 2**). We then doped the prepared BIT, with 5% in mass of MWNT. The Synthesis of MWNT was obtained by a chemical vapour deposition (CVD), using nickel as a precursor and using acetilene at 720°C. We added 5% in mass (0.25 g) of the MWNT to the 5 g BIT sample. The XRD for the MWNT, was too noisy, therefore, we decided to plot only the BIT + MWNT (5%) composite difratogram in **Figure 3**. The peak around 30o is still present (besides the others around 22°, 33° and 47° see **Figure 2**), however, the noise from the MWNT contributed to the graph in **Figure 3**.

### 2.1. Substrates and Electrodes

The samples were prepared in a disk shape (with thick-

**Table 1. Bit preparation.**

Paper	Milling	Calcination	Sinterization	$\rho$ (Kg/m <sup>3</sup> )
[19]	15 h/220 rpm	-----	850°C/1 h	7910
This work	4 × 10 min 370 rpm	850°C/20 min.	1020°C/1 h	7520

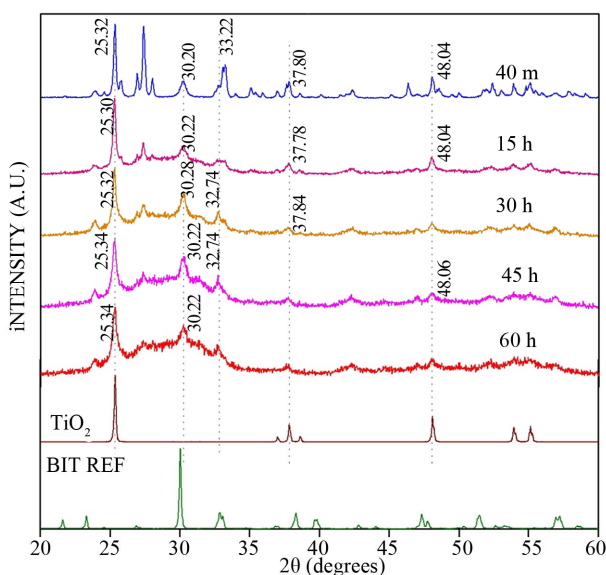


Figure 1. XRD for BIT milled for several times.

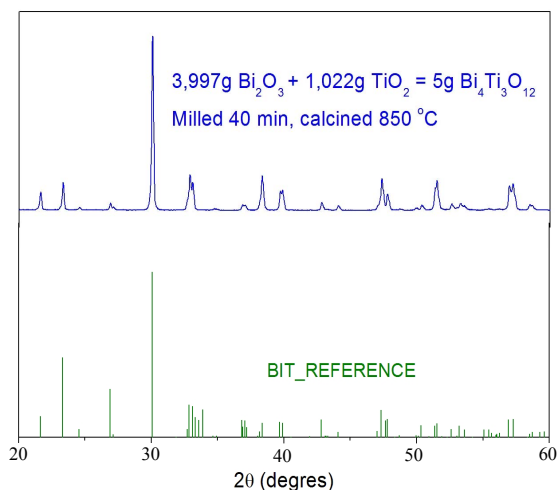


Figure 2. XRD for the calcined BIT.

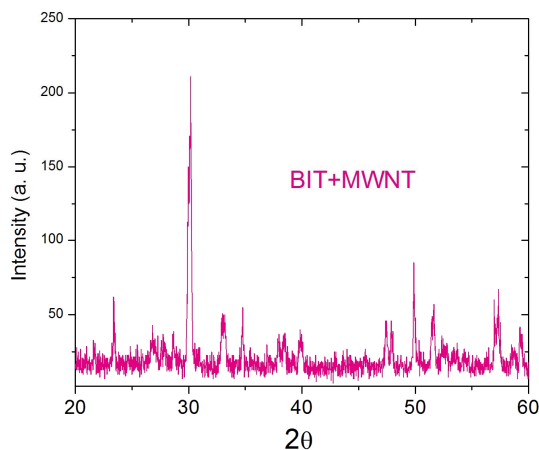


Figure 3. XRD for the BIT+MWNT composite.

ness around 1 mm). The circular electrodes were prepared using the screen printing technique (diameter around 10 mm) using silver (Ag) (Joint Metal-PC200).

## 2.2. X-Ray Diffraction

The X-ray diffraction (XRD) patterns were obtained under room temperature (300 K) by step scanning using powdered samples. We used 5s for each step of the counting time, with a  $\text{Cu-K}\alpha$  tube at 40 kV and 25 mA, using the geometry of Bragg-Brentano.

## 2.3. Dielectric Measurements

The Dielectric measurements were obtained from a HP 4291A Material Impedance Analyzer in conjunction with a HP 4194 Impedance Analyzer, which jointly covered the region of 100 Hz - 1.8 GHz in room temperature (300 K).

## 2.4. Infrared Spectroscopy

The infrared spectra (IR) were measured using KBr pellets made from a mixture of powder for each sample. The pellet's thickness varied from 0.5 - 0.6 mm. The IR spectra were measured from 400 - 1600  $\text{cm}^{-1}$  with a Nicolet 5ZPX FT-IR spectrometer.

## 2.5. Raman Spectroscopy

The Raman spectra were collected with a triple-grating spectrometer in the subtractive mode with a JobinYvon, T64000 equipment. The 514.5 nm line of an Argon ion laser was used as excitation. Olympus microscope lenses with a focal distance  $f = 20.5$  mm and numeric aperture  $\text{NA} = 0.35$ , was used to focus the laser on the sample surface. In this study the slits were set for a resolution of about  $2 \text{ cm}^{-1}$ .

## 3. Results and Discussion

### 3.1. X-Ray Diffraction for the Pure BIT, and BIT + MWNT

Figure 1 shows the X-ray diffraction (XRD) patterns of the milled samples with BIT together with the XRD of the reference (JCPDS), associated to  $\text{TiO}_2$  and BIT (BIT\_REF), which were used in the sample preparation (as discussed before). In this sample one can easily identify all the peaks associated to BIT and  $\text{TiO}_2$  phase. This particular sample BIT was calcined with 40min of ball milling and the presence of the  $\text{TiO}_2$ , which was still noted. Weak peaks around  $37.8^\circ$  and  $48.2^\circ$  could be detected. Regarding the sample, BIT calcined with 60min of ball milling, showed a weak presence of BIT. These results suggest that the ball milling process lead the grain

size reduction and leading to an amorphous phase.

An amorphization process after 15 h of milling is shown in **Figure 1**. We observed that with increasing milling time, the characteristic of the sample is predominantly amorphous. The peak around  $25^\circ$  is present at all times and it is associated with Mogae  $\text{TiO}_2$  [25,26]. The BIT in its orthorhombic phase was obtained by grinding procedure followed by calcination (as described above). The crystallite size was around 140 nm (using Scherrer equation). However, we had to vary the temperature from  $850^\circ\text{C}$  to  $1000^\circ\text{C}$  at a rate of rise and fall of  $5^\circ\text{C}/\text{min}$ . The pellets were pressed with 1 ton of discs in 12 mm by 0.6 mm of thickness on average. After pressing were fired for 20 minutes (or up to 1 hour) sintering.

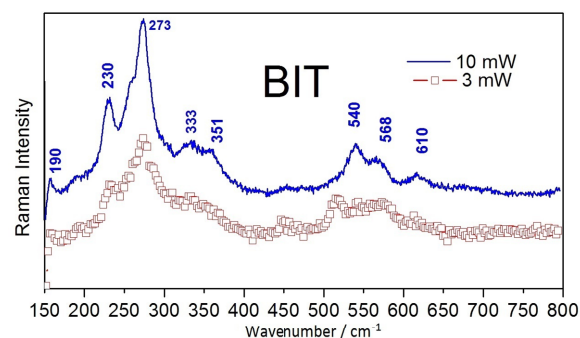
Hence, the calcined BIT 40 min sample for 20 min at  $850^\circ\text{C}$  (in order to eliminate traces of  $\text{TiO}_2$ ), sintered the pellet at  $1020^\circ\text{C}$  for 1h, shown on **Table 1**. The XRD for the calcined BIT and its reference is plotted in **Figure 2**. The calcined XRD duly showed perfect fitting with the BIT reference, while the same XRD pattern occurred in the sintered sample.

### 3.2. Raman Spectroscopy

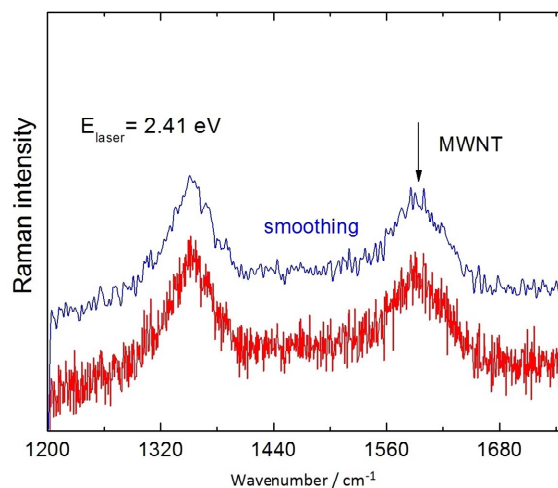
**Figure 4(a)** and **(b)** showed the Raman spectra of the BIT and MWNTs samples, respectively. **Figure 4(a)** showed the peaks located at 230 and  $273\text{ cm}^{-1}$ . These peaks are assigned [25] to vibrations of O-Ti-O. The Raman mode located at  $230\text{ cm}^{-1}$  is Raman-inactive, according to the symmetry rules of the octahedron  $\text{TiO}_6$ . However, it is observed that due to the distortion of the octahedron, the mode at  $333\text{ cm}^{-1}$  is a combination of vibration modes, being stretching and bending modes. The vibration modes at  $540\text{ cm}^{-1}$  correspond to the excursions of peak oxygen octahedron. The octahedron  $\text{TiO}_6$  showed considerable distortion, therefore, some Raman modes located at 333, 540 and  $612\text{ cm}^{-1}$ , appeared broad and weak, which may induce dielectric anomalies [25]. **Figure 4(c)** showed a similar pattern to that of pure BIT (**Figure 4(a)**), however, with fewer spikes. Note the values of  $273\text{ cm}^{-1}$ ,  $333\text{ cm}^{-1}$  and  $540\text{ cm}^{-1}$ , as well as the attenuation of the peaks at  $190\text{ cm}^{-1}$  and  $230\text{ cm}^{-1}$ . We conclude that the ball milling process leads the MWNT (**Figure 4(b)**) disappearance of these duly stated peaks in the composite.

In carbon nanotubes and related materials, the D and G bands of the Raman vibrational, involves the stretching and the bending of C-C bonds. The G modes are related with the in-plane vibrational ( $E_{2g}$ ) movement of carbon atoms and the D-band Raman vibrational mode ( $A_{1g}$ ), due to the collective in-plane vibrational movement of the atoms, towards and away from the center of the hexagons formed by the covalently ( $sp^2$ ) bonded carbon atoms. The MWNT Raman spectra are shown in **Figure**

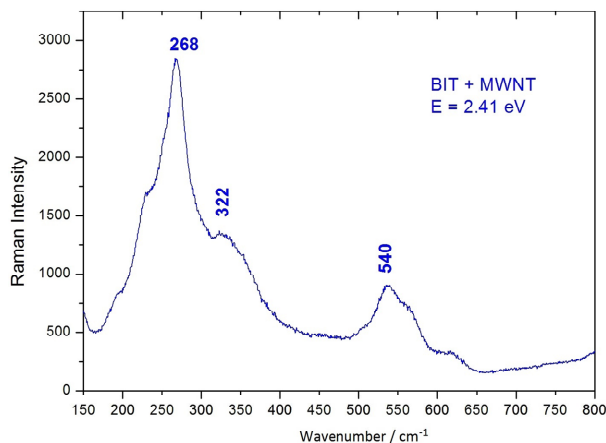
**4(b)**. They are consisted of the main G band at about  $1580\text{ cm}^{-1}$  (C-C stretching vibrations) and two disorder-induced bands-D at about  $1340\text{ cm}^{-1}$  and D', at about  $1620\text{ cm}^{-1}$  reflecting the high density of states for zone-edge and midzone phonons, respectively [27].



(a)



(b)



(c)

**Figure 4.** (a) Raman spectra of the BIT and MWNT. (b) Raman spectra of the MWNT. (c) Raman spectra of the BIT + MWNT.

### 3.3. Infrared Spectroscopy

The infrared spectra of the BIT, MWNT and BIT + MWNT, are shown in **Figure 5**. All absorptions are stretchings of Ti-O, below 405 cm<sup>-1</sup>, thus, having a bending absorption of Ti-O. Our results agree with the orthorhombic phase [25-28]. On **Table 2**, we can note the IR vibrations modes for the BIT. They agree with the literatures [12,13]. In **Figure 5** there is a dramatic change in the infrared spectrum. An absorption at 817 cm<sup>-1</sup> is still present, however, there is a total change in the spectrum of **Figure 5**.

### 3.4. Dielectric Measurements

After several tests, the measurements emerged as the ideal stage, represented by the BIT **Figure 2**. This led us to perform measurements of the dielectric constant. The procedure was to apply the silver electrodes, using the technique of the “screen printing” on both sides and drying the deploy connect wires afterwards as shown in

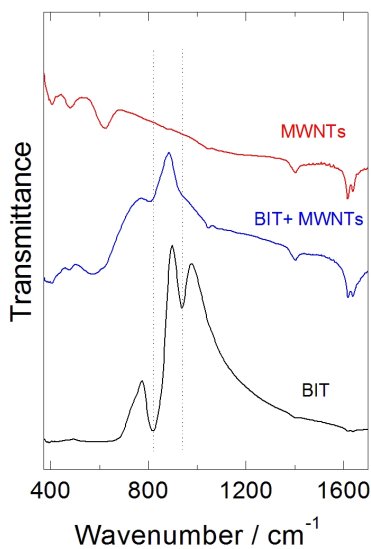


**Figure 5.** Infrared spectra of the BIT, MWNT and BIT + MWNT.

**Table 2.** Assignment of the Raman modes

Raman modes(cm <sup>-1</sup> )	BIT	BIT + MWNT	Papers [26][27]
(Ti-O)(ss)	476 w, 590 vs, 817 s, 958 w, 1062 w	476w, 590vs, 817s, 958w, 1062w	476w, 590vs, 817s, 958w, 1062w
(Peaks in figures)	192, 229, 267, 338, 536, 564, 618, 852 (Figure 4(a))	268, 322, 540 (Figure 4(c))	

**Figure 6**. The model adopted to measure the capacitance, was from a parallel plate capacitor, in which it used the expression (1). Where Co is the capacitance, measured in an HP 4194 impedancimeter ranging from 100 Hz to 40 MHz, and the thickness of the tablet in meters, A the area of the silver electrode and ε<sub>o</sub> the vacuum permittivity .

$$K = \frac{C_o \epsilon}{\epsilon_o A} \therefore \quad (1)$$

**Figure 6** shows the dielectric constant measurements of the BIT and BIT + MWNT, respectively. In **Figure 6**, we note the smooth curve for the pure BIT, with a dielectric constant of 288.11 at 100 Hz. This constant drops smoothly around 150 at 100 kHz. We can notice also that for the BIT + MWNT sample, the dielectric constant decreases so fast starting from 468.30 at 100 Hz to a dramatic dropping around 100 at 100 kHz. On **Table 3** we have some values for both dielectric constant and loss.

We can notice as well in **Figure 7**, that the greatest loss is of 0.24 around 100 Hz for the pure BIT, we also note that the smooth curve leads to a value of 0.027 at 100 kHz. Furthermore, the BIT + MWNT have shown a dramatic change values from 0.43 at 100 Hz to 0.076 at 100 kHz. In terms of the dielectric losses and dielectric

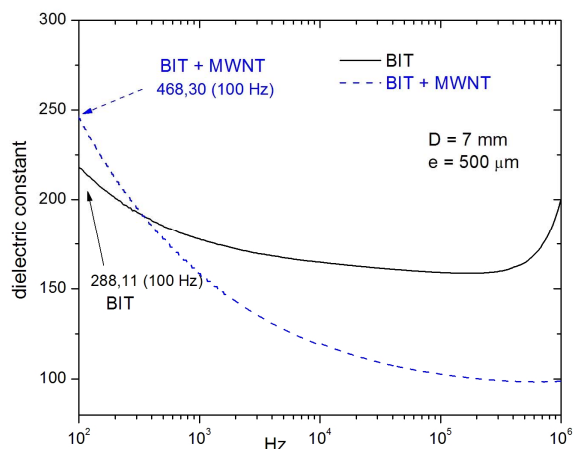


**Figure 6.** BIT and BIT + MWNT dielectric constants versus frequency. The model adopted to measure the capacitance was that of a parallel plate capacitor in which he used the expression (1).

**Table 3.** Dielectric constant and loss versus frequency.

Composite	K	K	K	K
	D	D	D	D
	(100 Hz)	(1 kHz)	(100 kHz)	(1 MHz)
BIT	288,1 0,24	217,4 0,10	159,0 0,027	200,62 0,058
BIT + MWNT	468,30 0,43	158,54 0,28	102,76 0,076	98,79 0,039

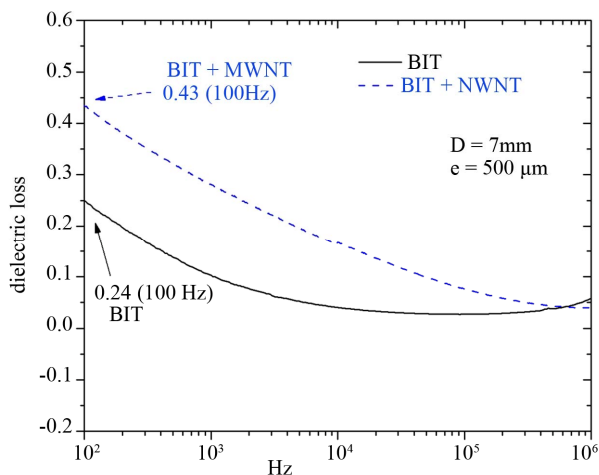


**Figure 7. Dielectric loss versus frequency for the pure BIT and BIT + MWNT.**

constant, the pure BIT is best for low frequencies. The nanotube BIT composite is the best for high frequencies.

#### 4. Conclusion

In summary, nano-sized bismuth titanate  $\text{Bi}_4\text{Ti}_3\text{O}_{12}$  (BIT) powders, were prepared by a high-energy ball milling process from their oxide mixture of  $\text{Bi}_2\text{O}_3$  with  $\text{TiO}_2$ . After the preparation of the above said compound ( $\text{Bi}_4\text{Ti}_3\text{O}_{12}$ ), it was doped with Multi Walled Carbon Nanotubes obtained by a chemical vapour deposition (CVD) and preceded with the dielectric and optical measurements. The dielectric constant measurements of the BIT and BIT + MWNT, show that for all the samples, the dielectric constant always decreases with the increase of the frequency until 15 MHz. Furthermore, around 17 MHz, we noticed that there was a resonance like behavior in the BIT + MWNT composite. This aforesaid behavior was understood to be related to the ball milling process, which leads the MWNT changes in the optical properties on BIT + MWNT.

#### 5. Acknowledgements

We would like to thank to the institution below: UFC, LOCEM, UECE, CNPq, CAPES, FUNCAP, G.D. Saraiva acknowledges the support from MCT/CNPq Edital 14/2010 (process 476569/2010-9), FUNCAP/Edital 02/2010 (process 10293648-0) and FUNCAP/Edital 05/2009 (process 186.01.00/09). The other authors acknowledge CNPq and FUNCAP for partial financial support.

#### REFERENCES

- [1] I. F. Dorrian, R. E. Newnham and K. K. Smith, "Crystal Structure of  $\text{Bi}_4\text{Ti}_3\text{O}_{12}$ ," *Ferroelectrics*, Vol. 3, No. 1, 1971, pp. 17-27. [doi:10.1080/00150197108237680](https://doi.org/10.1080/00150197108237680)
- [2] S. E. Cummings and L. E. Cross, "Electrical and Optical Properties of Ferroelectric  $\text{Bi}_4\text{Ti}_3\text{O}_{12}$  Single Crystals," *Journal of Applied Physics*, Vol. 3, No. 5, 1968, pp. 2268-2274. [doi:10.1063/1.1656542](https://doi.org/10.1063/1.1656542)
- [3] H. S. Shulman, M. Testorf, D. Damjanovic, N. Setter and M. Crostructure, "Electrical Conductivity and Piezoelectric Properties of Bismuth Titanate," *Journal of the American Ceramic Society*, Vol. 79, No. 12, 1996, pp. 3214-3218.
- [4] M. Villegas, A. C. Caballero, C. Moure and P. Duran, "Factors affecting the electrical conductivity ~ donor-doped  $\text{Bi}_4\text{Ti}_3\text{O}_{12}$  piezoelectric ceramics," *Journal of the American Ceramic Society*, Vol. 82, No. 9, 1999, pp. 2411-2416.
- [5] A. Q. Iiang, H. G. Li and L. D. Zhang, "Dielectric Study Inanocrystalline Prepared by Chemical Doprecipitation," *Journal of Applied Physics*, Vol. 83, No. 9, 1998, pp. 4878-4883. [doi:10.1063/1.367287](https://doi.org/10.1063/1.367287)
- [6] S. H. Hong, I. A. Horn, S. Trolier-McKinstry and G. L. Messing, "Dielectric and Ferroelectric Properties of Ta-Doped Bismuth Titanate," *Journal of Materials Science Letters*, Vol. 19, No. 18, 2000, pp. 1661-1664. [doi:10.1023/A:1006722312423](https://doi.org/10.1023/A:1006722312423)
- [7] I. A. Horn, S. C. Zhang, U. Selvaraj and G. L. Messing, Trolier-McKinstry, Templated Grain Growth of Textured Bismuth Titanate," *Journal of the American Ceramic Society*, Vol. 82, No. 4, 1999, pp. 921-926. [doi:10.1111/j.1151-2916.1999.tb01854.x](https://doi.org/10.1111/j.1151-2916.1999.tb01854.x)
- [8] T. Takeuchi, T. Tani and Y. Saito, "Unidirectionally Texture  $\text{CaBi}_4\text{Ti}_4\text{O}_5$  Ceramics by the Reactive Templated Grain Growth with an Extrusion," *Japanese Journal of Applied Physics*, Vol. 39, 2000, pp. 5577-5584. [doi:10.1143/JJAP.39.5577](https://doi.org/10.1143/JJAP.39.5577)
- [9] P. S. Gilman and I. S. Benjamin, "Mechanical Alloying," *Annual Review of Materials Research*, Vol. 13, 1983, pp. 279-300. [doi:10.1146/annurev.ms.13.080183.001431](https://doi.org/10.1146/annurev.ms.13.080183.001431)
- [10] I. Z. Iiang, F. W. Poulsen and S. Morup, "Structure and Thermal Stability of Nanostructured Iron-Doped Zirconia Prepared by High-Energy Ball Milling," *Journal of Materials Research*, Vol. 14, No. 4, 1999, pp. 1343-1352. [doi:10.1557/JMR.1999.0183](https://doi.org/10.1557/JMR.1999.0183)
- [11] J. Z. Iiang, R. Lin, W. Lin, K. Nielsen, S. Morup, K. DamJohansen and R. Clasen, "Gas-Sensitive Properties and Structure of Nanostructured  $(\alpha\text{-Fe}_2\text{O}_3)_x(\text{SnO}_2)_x$  Materials Prepared by Mechanical Alloying," *Journal of Physics D: Applied Physics*, Vol. 30, No. 10, 1997, pp. 1459-1467. [doi:10.1088/0022-3727/30/10/012](https://doi.org/10.1088/0022-3727/30/10/012)
- [12] M. Simoneau, G. L. Esperance, M. L. Trudeau and R. Schulz, "Structural and Magnetic Characterization of Granular  $\text{Yb}_2\text{Cu}_3\text{O}_7$  nanocrystalline Powder," *Journal of Materials Research*, Vol. 9, No. 3, 1994, pp. 535-540. [doi:10.1557/JMR.1994.0535](https://doi.org/10.1557/JMR.1994.0535)
- [13] G. Nicoara, D. Fratiloiu, M. Nogues, J. L. Dormann, F. Vasiliu, "Ni-Zn Ferrite Nanoparticles Prepared by Ball Milling," *Materials Science Forum*, Vol. 235-238, No. 1, 1997, pp. 145-150. [doi:10.4028/www.scientific.net/MSF.235-238.145](https://doi.org/10.4028/www.scientific.net/MSF.235-238.145)
- [14] J. Xue, D. Wan, S. E. Lee and I. Wang, "Mechanochemical Synthesis of Lead Zirconatetitanate from Mixed Ox-

- ides,” *Journal of the American Ceramic Society*, Vol. 82, No. 7, 1999, pp. 1687-1692.  
[doi:10.1111/j.1151-2916.1999.tb01987.x](https://doi.org/10.1111/j.1151-2916.1999.tb01987.x)
- [15] L. B. Kong, W. Zhu and O. K. Tan, “Preparation and Characterization of  $\text{Pb}(\text{ZrO}_5\text{TiO}_4)\text{O}_3$  Ceramics from High-Energy Ball Milled Powders,” *Materials Letters*, Vol. 42, No. 4, 2000, pp. 232-239.  
[doi:10.1016/S0167-577X\(99\)00190-1](https://doi.org/10.1016/S0167-577X(99)00190-1)
- [16] J. Wang, I. Xue, D. Wan and W. Ng, “Mechanochemical Fabrication of Single Phase PMN of Perovskite Structure,” *Solid State Ionics*, Vol. 124, No. 3-4, 1999, pp. 271-279.
- [17] M. Villegas, A. C. Caballero, C. Moure, P. Duran, J. F. Fernandez and R. E. Newnham, “Influence of Processing Parameters on the Sintering and Electrical Properties of  $\text{Pb}(\text{Zn}_{1/3}\text{Nb}_{2/3})\text{O}_3$ -Based Ceramics,” *Journal of the American Ceramic Society*, Vol. 83, No. 1, 2000, pp. 141-146.  
[doi:10.1111/j.1151-2916.2000.tb01162.x](https://doi.org/10.1111/j.1151-2916.2000.tb01162.x)
- [18] B. Z. Tian, X. L. Zheng, T. J. Kempa, Y. Fang, N. F. Yu, G. H. Yu, J. L. Huang and C. M. Lieber, “Coaxial Silicon Nanowires as Solar Cells and Nanoelectronic Power Sources,” *Nature*, Vol. 449, No. 7164, 2007, pp. 885-888.  
[doi:10.1038/nature06181](https://doi.org/10.1038/nature06181)
- [19] A. Javey, S.-W. Nam, R. S. Friedman, H. Yan and C. M. Lieber, “Layer-By-Layer Assembly of Nanowires for Three-Dimensional, Multifunctional Electronics,” *Nano Letter*, Vol. 7, No. 3, 2007, pp. 773-777.
- [20] A. G. Pinheiro, F. M. M. Pereira, M. R. P. Santos, H. H. B. Rocha and A. S. B. Sombra, “Electric Properties of  $\text{Bi}_4\text{Ti}_3\text{O}_{12}$ (BIT)- $\text{CaCu}_3\text{Ti}_4\text{O}_{12}$  (CCTO) Composite Substrates for High Dielectric Constant Devices,” *Journal of Materials Science*, Vol. 42, No. 6, 2007, pp. 2112-2120.
- [21] Y.-II Kim; M. K. Jeon, “Combined Structural Refinement of  $\text{Bi}_4\text{Ti}_3\text{O}_{12}$  Using X-Ray and Neutron Powder Diffraction Data,” *Materials Letters*, Vol. 58, No. 12-13, 2004, pp.1889-1893.
- [22] L. B. Kong, J. Ma, W. Zhu and O. K. Tan, “Preparation of  $\text{Bi}_4\text{Ti}_3\text{O}_{12}$  Ceramics via a High-Energy Ball Milling Process,” *Materials Letters*, Vol. 51, No. 2, 2001, pp. 108-114. [doi:10.1016/S0167-577X\(01\)00274-9](https://doi.org/10.1016/S0167-577X(01)00274-9)
- [23] S. E. Cummings and L. E. Cross, “Electrical and Optical Properties of Ferroelectric  $\text{Bi}_4\text{Ti}_3\text{O}_{12}$  Single Crystals,” *Journal of Applied Physics*, Vol. 39, No. 5, 1968, pp. 2268-2274. [doi:10.1063/1.1656542](https://doi.org/10.1063/1.1656542)
- [24] A. Q. Jiang, H. G. Li and L. D. Zhang, “Dielectric Study in Nanocrystalline Prepared by Chemical Doprecipitation,” *Journal of Applied Physics*, Vol. 83, No. 9, 1998, pp. 4878-4883. [doi:10.1063/1.367287](https://doi.org/10.1063/1.367287)
- [25] W. L. Liua, H. R. Xia, H. Hand and X. Q. Wang, “Structural and Dielectrical Properties of Bismuth Titanate Nanoparticles Prepared by Metalorganic Decomposition Method,” *Journal of Crystal Growth*, Vol. 269, No. 3-4, 2004, p. 499.
- [26] Joint Committee on Powder Diffraction Standards (JCPDS), “International Center for Diffraction Data,” Newton Square, 1995.
- [27] P. T. C. Freire, V. Lemos, J. A. Lima Jr., G. D. Saraiva, P. S. Pizani, R. O.Nascimento, N. M. P. S. Ricardo, J. Mendes Filho and A. G. Souza Filho, “Pressure Effects on Surfactant Solubilized Single-Wall Carbon Nanotubes,” *Physica Status Solidi (b)*, Vol. 244, No. 1, 2007, pp. 105-109.
- [28] O. Yamaguchi, N. Maruyama and K. Hirota, “Formation and Characterization of Alkoxy-Derived  $\text{Bi}_4\text{Ti}_3\text{O}_{12}$ ,” *British Ceramic Transactions and Journal*, Vol. 90, 1991, pp. 111-113.